

Article

Design and Control of the Side Reactor Configuration for Production of Ethyl Acetate

Reui-Chiang Tsai, Jian-Kai Cheng, Hsiao-Ping Huang,
Cheng-Ching Yu, Yi-Shan Shen, and Ying-Tien Chen

Ind. Eng. Chem. Res., **2008**, 47 (23), 9472-9484 • Publication Date (Web): 30 October 2008

Downloaded from <http://pubs.acs.org> on November 28, 2008

More About This Article

Additional resources and features associated with this article are available within the HTML version:

- Supporting Information
- Access to high resolution figures
- Links to articles and content related to this article
- Copyright permission to reproduce figures and/or text from this article

[View the Full Text HTML](#)



ACS Publications

High quality. High impact.

Industrial & Engineering Chemistry Research is published by the American Chemical Society. 1155 Sixteenth Street N.W., Washington, DC 20036

Design and Control of the Side Reactor Configuration for Production of Ethyl Acetate

Reui-Chiang Tsai,[†] Jian-Kai Cheng,[†] Hsiao-Ping Huang,[†] Cheng-Ching Yu,^{*,†} Yi-Shan Shen,[‡] and Ying-Tien Chen[‡]

Department of Chemical Engineering, National Taiwan University, Taipei 106, Taiwan and Engineering Center, China Petrochemical Development Corporation, Ta-Sheh, Kaohsiung 815 Taiwan

Despite some potential advantages of reactive distillation (RD), reactive distillation may suffer from maintenance/design problems such as catalyst deactivation/replacement and equipment design. In this work, an alternative design, a side reactor configuration, is sought and the process of interest is production of ethyl acetate via esterification. The reactive distillation study by Tang et al. (2005) reveals that almost 90% conversion takes place in the column base of the RD. This naturally suggests a coupled reactor/distillation configuration where all of the catalyst is packed in the bottoms base, denoted as single-reactive tray reactive distillation (RD-SRT). This mitigates the maintenance problem associated with conventional RD. However, simulation results show that, with the same amount of catalyst loading, the SRT configuration cannot achieve the same performance as the RD (~93% conversion). Another alternative is adding external reactors to the SRT, and this is termed the side reactor configuration (SRC). A systematic design procedure is devised for the SRC design, and the objective function to be minimized is the total annual cost (TAC). The results show that the TAC of the SRC only increases by 5% as compared to that of the RD. A plantwide control structure is developed followed by process identification and controller tuning. The results show that reasonable control performance can be achieved using simple temperature control for the feed flow rate and feed composition disturbances.

1. Introduction

Reactive distillation (RD), combining reaction and separation units in a single unit, is sometimes a favorable design alternative to a conventional reactor/separation configuration. Despite having advantages including a simplified separation section, reduced equipment cost, and energy savings, the RD technology requires specific equipment designs to facilitate chemical reaction in reactive trays. This is seldom encountered in conventional distillation. For example, large catalyst holdup in the RD column for maximizing conversion may not be consistent with the requirement of a high interfacial area for good separation.¹ In addition to catalyst holdup, potential conflict between the reaction temperature and separation may make the RD less effective as shown by Kaymak and Luyben.^{2,3} Catalyst deactivation is another issue for the RD. Traditional methods to compensate for catalyst deactivation, i.e., adding excess catalyst or increasing the reaction temperature, are seldom feasible in the RD applications.⁴ Thus, in practice, one has to overcome design/maintenance problems associated with reactive distillation.

An alternative is to couple a distillation column with one or more external side reactors, in so-called side reactor configurations (SRC).^{2–7} External reactors are used as a substitute for reactive trays. In such a manner, the SRC not only overcomes the design/maintenance problem of the RD but also achieves, to a degree, the benefits of a simultaneous reaction and separation feature. The side reactor configuration has been applied to systems such as productions of TAME, MTBE, diisobutene, etc. Most of the literature examples focus on the quantitative design to obtain equally good performance as compared to RD. However, at a conceptual level, evolution of the SRC, e.g., number of side reactors, side streams withdraw, and return trays, etc., is much less clear.

* To whom correspondence should be addressed. Tel.: +886-2-3366-3037. Fax: +886-2-2362-3040. E-mail: ccyu@ntu.edu.tw.

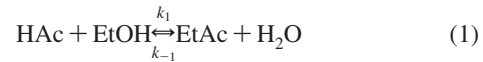
[†] National Taiwan University.

[‡] China Petrochemical Development Corporation.

The objective of this work is to investigate the design of the side reactor configuration for the reactive distillation where the reactive zone is placed at the lower section of the RD with no product removal from the column base. This configuration is called type II proposed by Tang et al.⁸ They explore steady-state design for acetic acid esterification with different alcohols (ranging from C1 to C5), which are categorized into three types of flow sheets. On the basis of the optimal RD design, optimally designed SRC evolves gradually after going through a transitional step. Production of ethyl acetate^{8,9} is used to illustrate the design procedure.

2. Process Description

The reaction for acetic acid (HAc) esterification with ethanol (EtOH) to produce ethyl acetate (EtAc) and water (H₂O) can be expressed as



The reversible reaction is described using a pseudohomogeneous model based on the mole fraction of component *i* (*x_i*) and catalyst weight (*m_{cat}*). Model parameters are taken from ref 10 for the esterification reaction catalyzed by Purolite CT179 ion-exchange resin. The rate expression can be written as

$$\begin{aligned} \mathcal{R} &= m_{\text{cat}} \times (k_F x_{\text{HAc}}^{1.5} x_{\text{EtOH}} - k_B x_{\text{EtAc}} x_{\text{H}_2\text{O}}) \\ k_F &= 4.24 \times 10^3 \exp\left(\frac{-48\ 300}{RT}\right) \\ k_B &= 4.55 \times 10^5 \exp\left(\frac{-66\ 200}{RT}\right) \\ K_{\text{eq}} &= 3.50 \quad (T = 350\text{K}) \end{aligned} \quad (2)$$

This corresponds to an exothermic reaction with an equilibrium constant slightly greater than 1. In process simulation, a catalyst density of 770 kg/m³ is assumed to calculate the total volume occupied by the catalyst in a reactive tray.

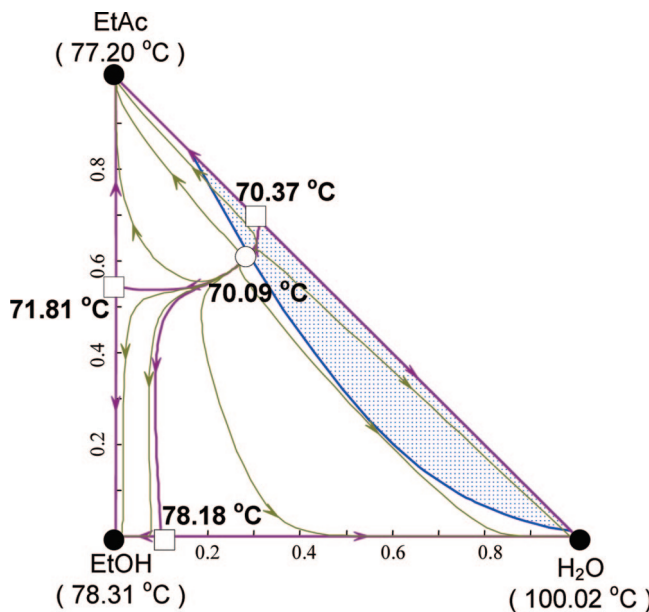


Figure 1. RCM diagram and two-liquid zone for the EtOH–EtAc–H₂O system.

To account for a nonideal vapor–liquid equilibrium (VLE) and possible vapor–liquid–liquid equilibrium (VLLE) for this quaternary system, the NRTL¹¹ model is used to calculate the activity coefficient, and model parameters are taken from Tang et al.⁸ Vapor-phase nonideality, dimerization of acetic acid, is also taken into consideration using the Hayden–O’Connell (HOC) second virial coefficient¹² model, and Aspen Plus built-in parameter values are used.

With the thermodynamic models available, the phase behavior can be predicted, and Table 1 shows the normal boiling point temperatures for pure components and azeotropic temperatures. The phase behavior exhibits a ternary minimum boiling azeotrope: ethanol, methyl acetate, and water at 70.09 °C (Figure 1). From the normal boiling point ranking, conceptually, this complex system can be viewed as a ternary system where two reactants, acetic acid and ethanol, can be treated as heavy key (HK) and intermediate key (IK), respectively; the ternary minimum-boiling azeotrope is considered as the product which the light key (LK). Thus, the reactive zone should be placed in the lower section of the RD column, while the pseudoproduct, liquid with an almost azeotropic composition, is removed from the top of the column overhead. This pseudoproduct is decanted, the water product is withdrawn from the aqueous phase, while the organic phase is further purified to obtain the acetate product. This is exactly the type II configuration of Tang et al.⁸

3. Conceptual Design

Figure 2 shows the RD flow sheet for EtAc production. The reactive zone is placed in the lower section of the RD column.

Table 1. Normal Boiling Point Ranking for Pure Components and Azeotropes

component/azeotrope	T (°C)
EtOH–EtAc–H ₂ O	70.09
EtOH–EtAc	71.81
EtOH–H ₂ O	78.18
EtAc	77.2
EtAc–H ₂ O	70.37
EtOH	78.31
H ₂ O	100
HAc	118.01

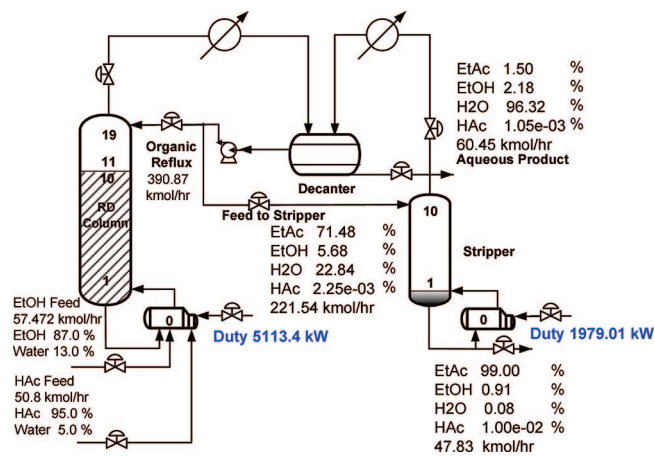


Figure 2. RD flow sheet of the EtAc production.

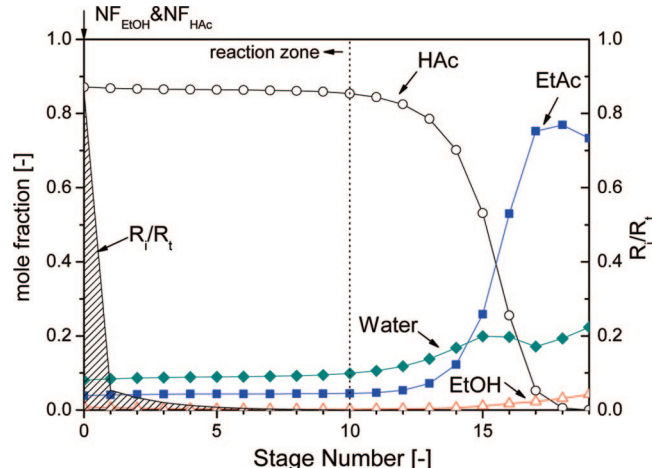


Figure 3. Composition profile in the RD column where the shaded area indicates the fraction of total conversion in each tray and close to 90% of the total conversion occurring in the column base.

The condensed overhead vapor from the RD column is decanted. The aqueous product is withdrawn from the decanter and the organic phase is split with a portion returned to the RD column and a portion fed to a stripping column which produces high-purity EtAc. In the RD column, because the column base has a much larger residence time than a tray, the catalyst holdup is the column base which is assumed to be 10 times of that on the reactive tray. The two fresh feeds into the RD are alcohol feed below azeotropic composition (87% EtOH and 13% H₂O) and industrial-grade acid feed (95 mol % HAc and 5% H₂O). Following the work of Lai et al.,⁹ the optimized flow sheet consists of a RD column and a stripper as shown in Figure 2. The flow sheet is obtained by minimizing the total annual cost (TAC)

$$\text{TAC} = \text{operating cost} + \frac{\text{capital cost}}{\text{payback time}} \quad (3)$$

Here, a payback time of 3 years is used. The operating cost includes the cost of steam, cooling water, and catalyst. The capital cost comprises the costs of the column, trays, and heat exchangers. Cost models and corresponding values are given in Appendix A (section 6). A catalyst life of 3 months is assumed.

The RD column has 10 reactive trays plus a reactive column base, 9 rectifying trays, and a decanter. The stripper column has 9 trays. Figure 3 shows the composition profile of the RD.

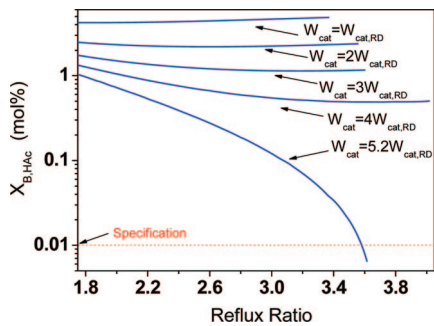


Figure 4. loading in the SRT configuration versus achievable acetic acid conversion under different reflux ratio.

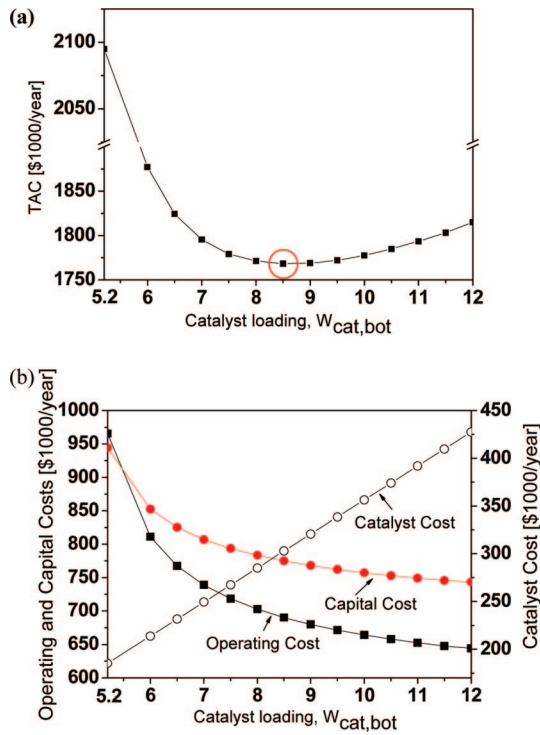


Figure 5. (a) Effect of catalyst loading in the column base ($W_{cat,bot}$) on TAC for the RD-SRT configuration and (b) trade off of operation cost (excluding catalyst cost), capital cost, and catalyst cost.

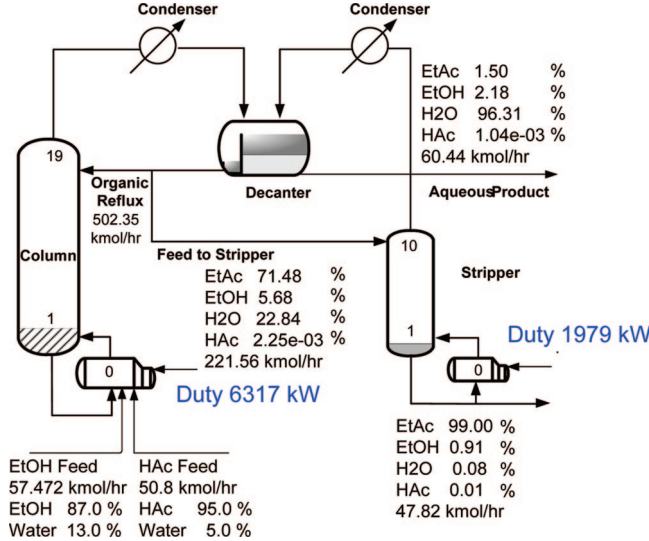


Figure 6. Optimized single reactive tray configuration (RD-SRT) for the EtAc production.

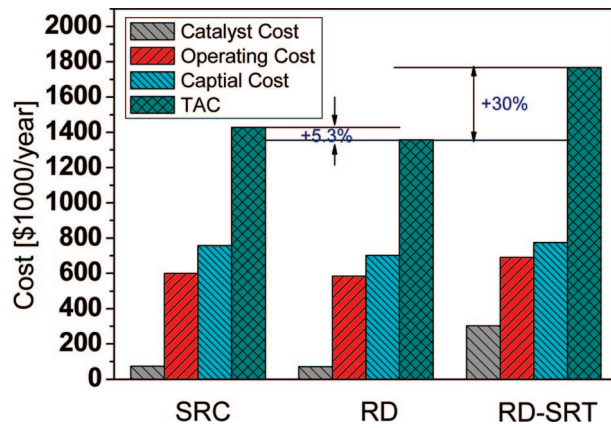


Figure 7. Comparison of TAC's for EtAc production using reactive distillation (RD), single reactive tray reactive distillation (RD-SRT), and side reactor configuration (SRC).

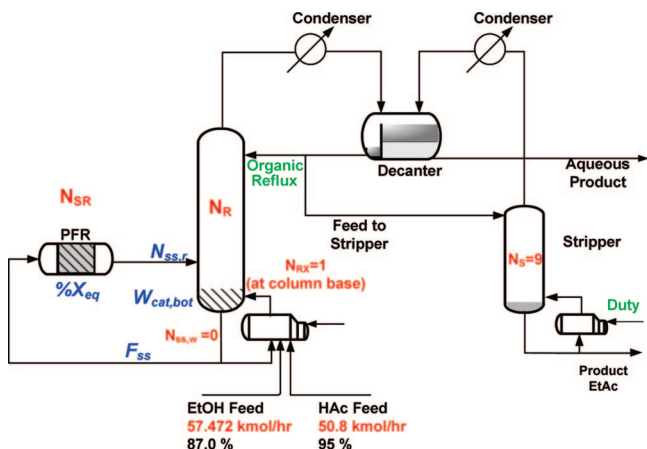


Figure 8. Side reactor configuration (SRC) with the design parameters indicated in italics.

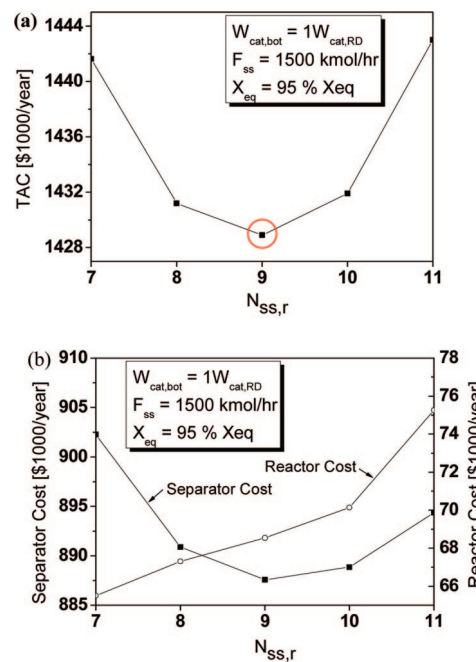


Figure 9. (a) Effect of side stream return tray ($N_{ss,r}$) on TAC's and (b) trade off of the separator cost (capital and operating costs) and reactor cost.

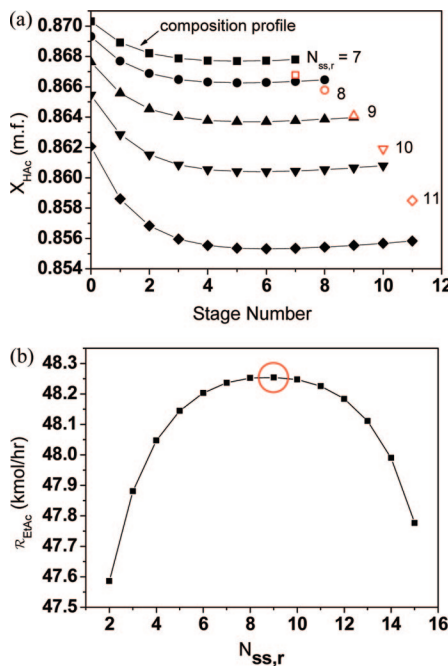


Figure 10. (a) Comparison of the HAc concentration at the side reactor effluent (open marker) and in the return tray (solid marker, composition profile in the column up to the return tray) as side stream return tray varied and (b) effect of side stream return tray ($N_{ss,r}$) on the total generation of EtAc.

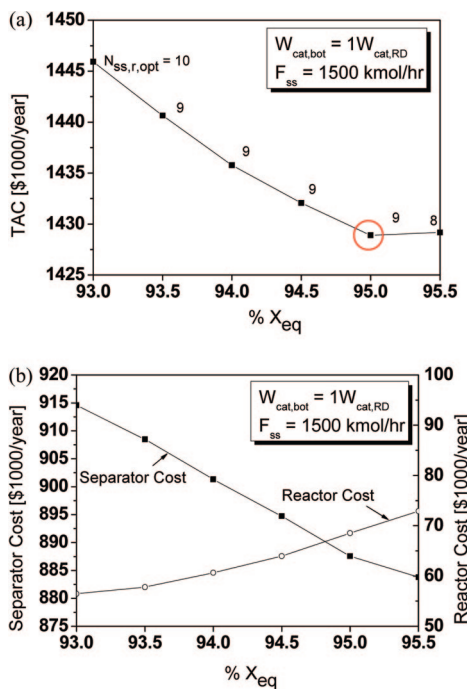


Figure 11. (a) Effects of percentage of equilibrium conversion (% X_{eq}) of the side reactor on TAC's and (b) trade off in the separator cost and reactor cost.

From now on, emphasis will be placed on the RD column and design alternatives will be sought while keeping the same design and product specifications for the stripper.

3.1. Single Reactive Tray (SRT). The composition profile in the RD column (Figure 3) reveals that the concentration of the heavy reactant (HAc) remains fairly constant (~90%) throughout the reactive zone, while the light reactant (EtOH) has a very low concentration in the column base (~1%) and the composition decreases toward the end of the reactive zone. More importantly, close to 90% of the total conversion occurs

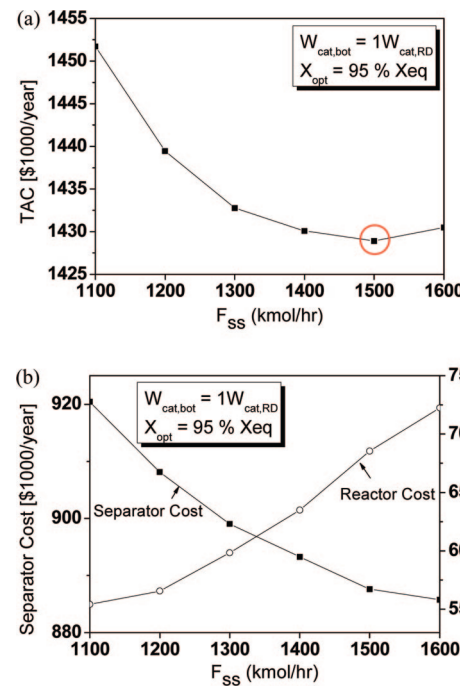


Figure 12. (a) Effect of side stream flow rate (F_{ss}) on TAC's and (b) trade off in the separator cost and reactor cost.

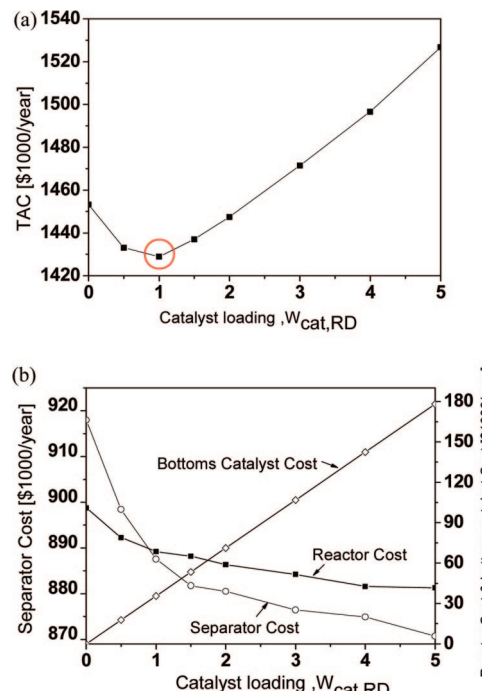


Figure 13. (a) Effect of catalyst loading in the column base ($W_{cat,bot}$) on TAC's and (b) trade off of the separator cost (excluding catalyst cost), reactor cost, and bottoms catalyst cost.

in the column base as shown in the shaded area in Figure 3. This naturally suggests a coupled reactor/separator configuration;^{13–15} that is, the single reactive tray (RD-SRT) configuration we can place all the catalyst in the column base and this becomes a single reactive tray column. The SRT configuration seems intuitively appealing and has the advantage of easy catalyst replacement. However, simulation results show that with the same catalyst weight as that of the RD column ($W_{cat,RD} = W_{cat,bot} + W_{cat,trays}$) the SRT configuration is unfeasible for the given purity specification. In fact, the required catalyst loading

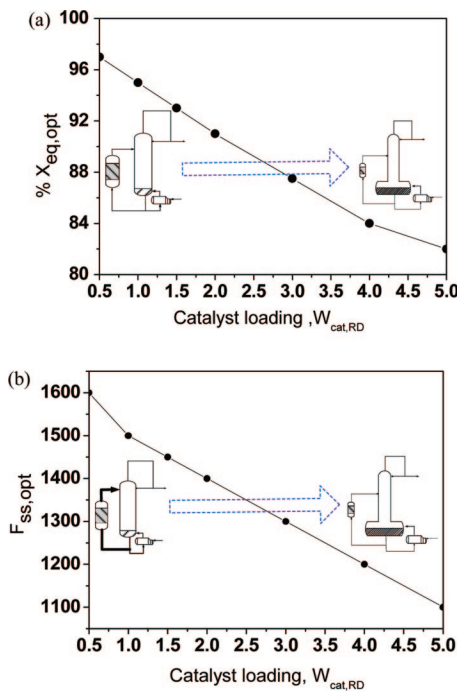


Figure 14. Relationships between design variables: (a) catalyst loading versus optimized percentage of equilibrium conversion (to achieve minimum TAC's) and (b) catalyst loading versus the optimized side stream flow rate (to achieve minimum TAC's).

is $5.2W_{cat, RD}$. Figure 4 clearly shows that the acid concentration at the column overhead cannot reach the specification unless a substantial increase in the catalyst loading is made. Thus, the performance of the SRT configuration is not as good as that of RD. The conversion is only 93% with the same catalyst loading ($W_{cat, RD}$) as opposed to 99% for RD. To obtain an improved design for the SRT configuration, the TAC is computed as the amount of catalyst in the column base ($W_{cat, bot}$) is varied. As expected, the catalyst holdup ($W_{cat, bot}$) increases, the capital and energy costs decrease, and the catalyst cost increases. The optimized SRT design gives a catalyst loading of $8.5W_{cat, RD}$, and the energy cost increases by 24% as shown in Figure 5. The improved SRT design is shown in Figure 6 with an organic

phase reflux ratio of 2.27 as opposed to 1.76 for the RD. The optimized SRT configuration has a TAC 30% greater than that of the RD configuration (Figure 7). The result reveals that despite having almost 90% conversion in the column base for the RD additional reaction stages are essential to achieve high-purity specification (i.e., high conversion) with acceptable capital and energy costs.

3.2. Side Reactor Configuration (SRC). If a second reaction stage should be included, the questions then become (1) what type of reaction system and (2) where should the reactor be placed? The answer to the first question is relatively simple: from a maintenance perspective, an external side reactor is preferred (compared to an internal one). The second question actually addresses two issues: (1) where should the side stream be withdrawn ($N_{ss,w}$ = feed to the side reactor) and (2) which is the side stream return tray ($N_{ss,r}$ = effluent from the side reactor)? The side stream is withdrawn from where the reactants are most abundant. For the EtAc production system this is from the column base. The selection of side stream return tray ($N_{ss,r}$) is less obvious, and it depends on other design parameters. In theory, finding the side stream return tray is analogous to finding the optimal feed tray location for a feed stream. However, in the SRC configuration this feed composition and column composition are interrelated. In other words, the side reactor effluent composition depends on the reactor size and reactor feed composition which are functions of side stream return tray.

Thus, the design variables include catalyst holdup ($W_{cat, bot}$) in the column base, side stream flow rate (F_{ss} = side reactor feed flow rate), percentage of equilibrium conversion (% X_{eq}) in the side reactor, and side stream (reactor effluent) return tray ($N_{ss,r}$) as shown in Figure 8. We assume that a reactor is an adiabatic PFR with an aspect ratio (length/diameter) of 5. A systematic design procedure is proposed to find the optimal configuration. All simulations are carried out in Aspen Plus using the RadFrac and RPlug modules.

Given the production rate and product specifications, the design steps are follows: (1) set the same total number of trays equal to that of the RD ($N_T = 19$); (2) withdraw side stream from the bottoms of the distillation column ($N_{ss,w} = 0$); (3) set the number of the side reactor to one ($N_{SR} = 1$); (4) guess catalyst holdup in the column base (e.g., $W_{cat, bot} = r_W W_{cat, RD}$,

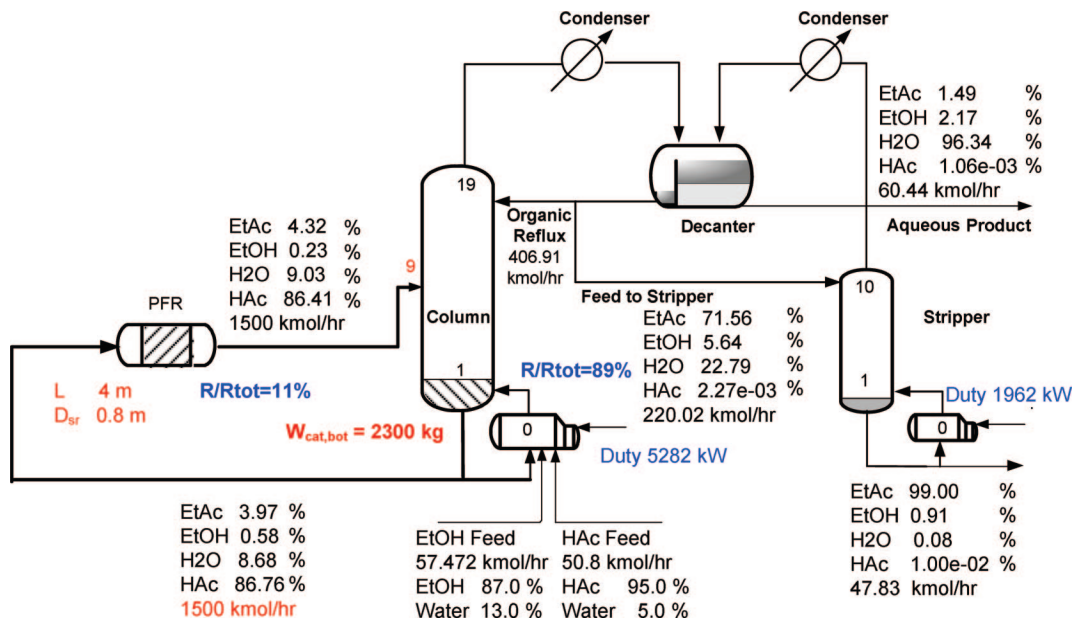


Figure 15. Optimized side reactor configuration (SRC) flow sheet for EtAc production.

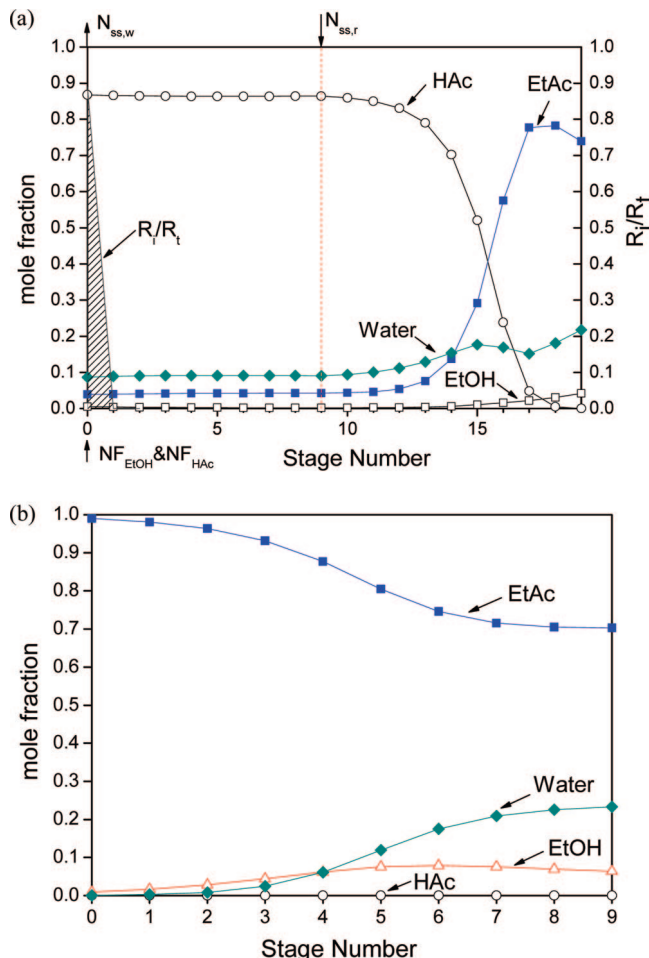


Figure 16. Composition profile in the SRC: (a) RD column where the shaded area indicates the fraction of total conversion in each tray and (b) stripping column.

which is a multiple of the initial total catalyst weight in the reactive distillation column); (5) guess a side stream flow rate (e.g., $F_{ss} = rR_{org}$, which is a multiple of the organic reflux flow rate); (6) guess the percent of the equilibrium conversion for the side reactor (e.g., $\%X_{eq} = 80\%$); (7) guess a side stream return tray ($N_{ss,r}$); (8) adjust the organic reflux ratio (R_{org}/D_{org}) until the HAc specification at the overhead (<100 ppm) is reached, adjust the stripper heat duty until the EtAc specification at the stripper bottoms (>99 mol %) is achieved, and adjust reactor size until the $\%X_{eq}$ is achieved; it is much easier to perform this in a sequential manner; (9) go back to 7 and change $N_{ss,r}$ until the TAC is minimized; (10) go back to 6 and change $\%X_{eq}$ until the TAC is minimized; (11) go back to 5 and change F_{ss} until the TAC is minimized; (12) go back to 4 and change $W_{cat,bot}$ until the TAC is minimized.

3.2.1. Effects of Side Stream Return Tray $N_{ss,r}$. Figure 9a shows that $N_{ss,r} = 9$ corresponds to the minimum TAC. The trade off comes from the reactor cost and separator cost, as shown in Figure 9b. The side stream is a large flow consisting of reactants and products (90 mol % HAc). From the separation cost point of view, it is optimal to feed the effluent from the side reactor onto a tray with a similar composition. On the other hand, moving the return tray location upward leads to a decrease in acetic acid concentration, as shown in Figure 10a, so the side reactor needs a larger reactor volume and more catalyst. In Figure 10 we observe that (1) the optimal return tray for the side reactor effluent is the tray with the liquid composition closest to that of the effluent and (2) the production rate of the

EtAc is at its maximum when $N_{ss,r} = 9$. Note that the tray number is counted from the bottom up.

3.2.2. Effects of Achieving Percentage of Equilibrium Conversion, $\%X_{eq}$. Figure 11a shows that $\%X_{eq} = 95$ is the optimal conversion. Again, we look at the reactor cost and separator cost, as shown in Figure 11b. As $\%X_{eq}$ increases, the reactor cost increases monotonically due to larger reactor volume and more catalyst needed for the additional reaction. At the same time, the separator cost decreases due to less reaction in the column base.

3.2.3. Effects of Side Stream Flow Rate, F_{ss} . Figure 12a shows that $F_{ss} = 1500$ (kmol/h) is the optimal side stream flow rate. A larger flow rate of the side stream requires a larger reactor volume and more catalyst to achieve the same conversion, so it leads to an increase in the reactor cost, as shown in Figure 12b. Because more reaction in the side reactor reduces the loading of the column, the separator cost decreases.

3.2.4. Effects of Catalyst Loading at Column Base, $W_{cat,bot}$. Figure 13a shows that $W_{cat,bot} = W_{cat,RD}$ is the optimal catalyst amount. As the bottoms catalyst increases, more reaction will occur in the column base. Therefore, the separator and side reactor need a smaller vapor flow rate and lower reactor volume, respectively. The trade off is shown in Figure 13b. If there is no catalyst in the column base ($W_{cat,bot} = 0$), i.e., only a side reactor for the reaction, this configuration can still work. However, it requires a larger flow rate of the side stream and a considerable amount of catalyst to achieve the product specification.

In summary, all of the trade off comes from the competition between the reaction in the column base and the side reactor. If we increase the reaction in the column base, it will reduce the loading of the side reactor and consequently the side reactor will require a smaller side stream flow rate and a lower percentage of equilibrium conversion, as shown in Figure 14.

For the case of one side reactor, the TAC only increases by a factor of 5% as compared to that of the RD design and we conclude that an additional external reactor will not be necessary for the SRC. Specifically, the energy cost of the SRC increases by a factor of 3% while using 1.67 times the amount of catalyst, as compared to the RD process. Figure 15 shows the optimized flow sheet where the side stream flow rate is 3.69 times the organic reflux flow rate and the catalyst loading in the column base and side reactor are $W_{cat,bot} = W_{cat,RD}$ and $W_{cat,SR} = 0.67W_{cat,RD}$. This corresponds to 95% of the equilibrium conversion for the side reactor. Moreover, 89% of the total conversion occurs in the column base, while the remaining 11% happens in the side reactor. Composition profiles for the SRC process are given in Figure 16. Figure 16 shows that the composition profile of the SRC is almost the same as that of the RD (c.f. Figure 3). Parameter values of steady-state designs of all three configurations (RD, SRT, and SRC) are summarized in Table 2.

4. Process Dynamics and Control

The number of studies on the control of reactive distillation columns has grown steadily in the past decade. Luyben and co-workers propose eight control structures for the “neat” reactive distillation of the ideal system (A + B \leftrightarrow C + D) (CS1-CS6 in Al-Arfaj and Luyben;¹⁶ CS6-CS7 in Al-Arfaj and Luyben,¹⁷ CS7-CS8 in Kaymak and Luyben).^{18,19} Hung et al.²⁰ explore control structure design for acetic acid esterification with different alcohols (ranging from C1 to C5), which are categorized into three types of flow sheets. As for control of various coupled reactor/column systems, some papers have been

Table 2. Parameter Values of Steady-State Designs (RD, RD-SRT, and SRC)

flow sheet	RD		RD-SRT		SRC	
	column configuration	RD	stripper	column	stripper	column
total no. of trays including reboiler	20	10	20	10	20	10
no. of trays in stripping section (N_S)		9		9		9
no. of trays in reactive section (N_{RX})	11		1		1	
no. of trays in rectifying section (N_R)	9		19		19	
reactive tray	0–10		0		0	
acetic acid feed tray	0		0		0	
alcohol feed tray	0		0		0	
feed flow rate of acid (kmol/h)	50.80		50.80		50.80	
feed flow rate of alcohol (kmol/h)	57.47		57.47		57.47	
top product flow rate (kmol/h)	60.45		60.44		60.443	
bottom product flow rate (kmol/h)		47.82		47.83		47.83
$X_{D,aq}$						
m.f. acid	0.00001		0.00001		0.00001	
m.f. alcohol	0.02182		0.0218		0.0217	
m.f. acetate	0.01498		0.015		0.0149	
m.f. water	0.96391		0.9631		0.9619	
X_B						
acid in ppm		100		100		100
m.f. alcohol		0.0091		0.0091		0.0091
m.f. acetate		0.9900		0.99		0.99
m.f. water		0.0008		0.0008		0.0008
condenser duty (kW)	-4789.92	-1668.7	-5845.6	-1669	-4941.3	-1653.9
subcooling duty (kW)	-881.45		-1030.0		-901.2	
reboiler duty (kW)	5113.4	1979.1	6316.9	1979.4	5282.5	1962.4
column diameter (m)	2.043	1.37	2.35	1.37	2.27	1.36
Weir height (m)	0.1016	0.0508	0.1016	0.0508	0.1016	0.0508
decanter temperature (°C)	40		40		40	
side reactor diameter (m)					0.8	
side reactor length (m)					4	
condenser heat transfer area (m ²)	177.1	61.9	215.6	61.9	182.6	61.3
subcooling heat transfer area (m ²)	179.96		210.3		183.99	
reboiler heat transfer area (m ²)	190.7	83.7	235.6	83.7	196.9	82.9
total capital cost (\$1000)	2103.0		2325.0		2269.3	
column	521.4		583.7		566.1	
reactor	0		0		90.1	
column trays	91.42		109.3		104.2	
heat exchangers	1490.2		1632.1		1508.3	
total operating cost (\$1000/year)	656.10		993.2		672.5	
catalyst cost	71.30		302.8		73.9	
energy cost	584.90		690.3		598.6	
TAC (\$1000/year)	1357.12		1768.16		1428.89	

presented.^{13–15,21,22} However, control of the side reactor configuration has not been discussed in the literature. In this section, a systematic approach to design the control structure is suggested. The design steps are as follows: (1) determine manipulated variables; (2) use NRG (nonsquare RGA) to determine temperature control trays; (3) use decentralized PI controller; (4) use RGA (relative gain array) for variable pairing; (5) use relay feed back to find K_u and P_u ; (6) use TL (Tyreus–Luyben) tuning to find controller settings.

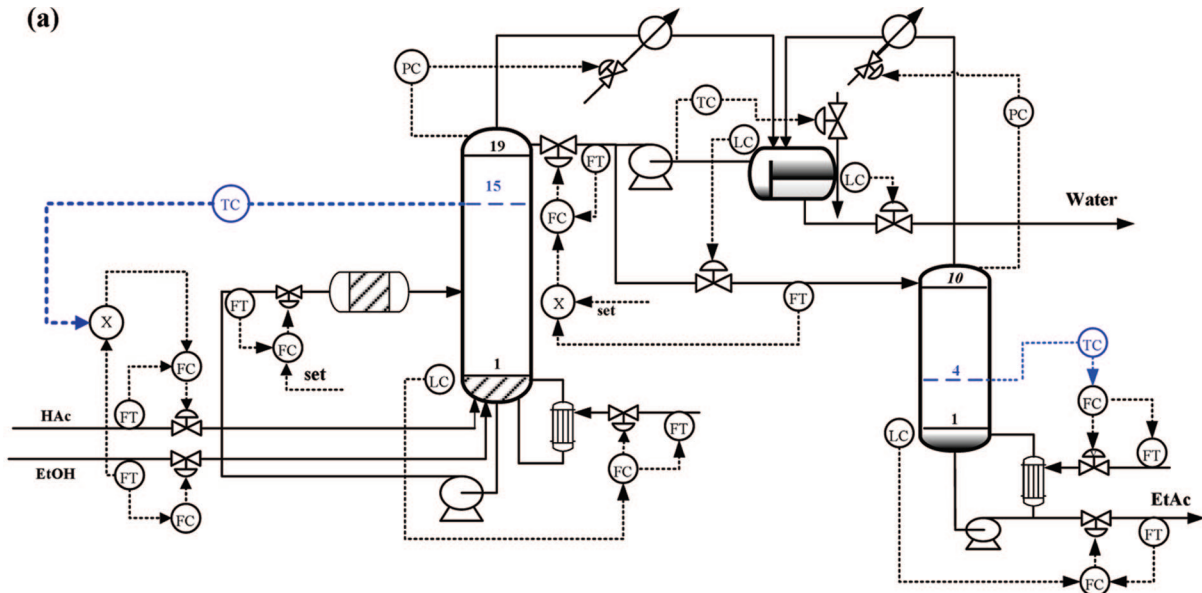
4.1. Determining Manipulated Variables. As compared to reactive distillation, the side reactor configuration (SRC) has one extra manipulated variable, side stream flow rate (F_{SS}), in addition to two feed flows (F_{EtOH} and F_{HAc}), two reboiler duties ($Q_{R,RD}$ and $Q_{R,STR}$), two condenser duties and one subcooling duty, aqueous and organic distillate flow rates, organic reflux flow rate (R), and stripper bottoms flow rate. Similar to the control of the reactive distillation system, the alcohol feed flow is selected as the throughput manipulator and we are left with 11 manipulated variables.

In this EtAc-SRC process there are six inventory control loops required, which include control of four levels (the RD column base level, the organic phase level in the decanter, the aqueous-phase holdup in the decanter, and the stripper base level) and

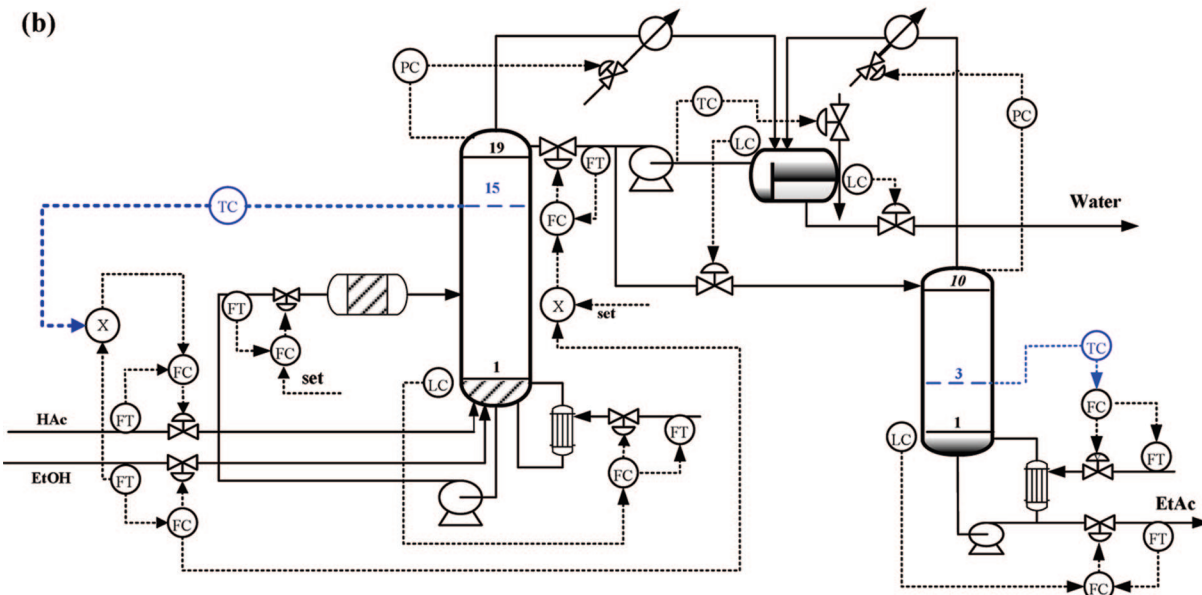
two column pressures of the RD and stripping columns. Basic inventory and related loops are arranged in the following ways. Top pressures of two columns are controlled by manipulating the condenser duties. The decanter temperature is controlled by changing the chilled water flow. As for liquid inventories, except for the RD column base the remaining liquid levels are controlled by their liquid outlet flow as shown in Figure 17. For the RD column base level control we have three candidates: side draw flow (F_{SS}), organic reflux flow (R), and reboiler duty ($Q_{R,RD}$). Because the side draw flow has zero-gain effect on the base level and the organic reflux flow gives slow dynamics,²² we choose the heat input of the RD column ($Q_{R,RD}$) to control the base level. In doing this, we have four manipulated variables left: F_{SS} , F_{HAc} , R , and $Q_{R,STR}$.

After selecting the inventory controls, the remaining manipulated variables (HAc feed, organic reflux flow, and stripper heat duty) are used for maintaining stoichiometric balance and quality control: purity of the ethyl acetate and water. In the stripper the acetate product purity is controlled by the stripper heat input ($Q_{R,STR}$) and temperature is used to infer the product composition. From the RCM (Figure 1) the water purity is determined by the tie line of the liquid–liquid equilibrium, so it is left uncontrolled. In order to maintain the stoichiometric balance,

(a)



(b)



(c)

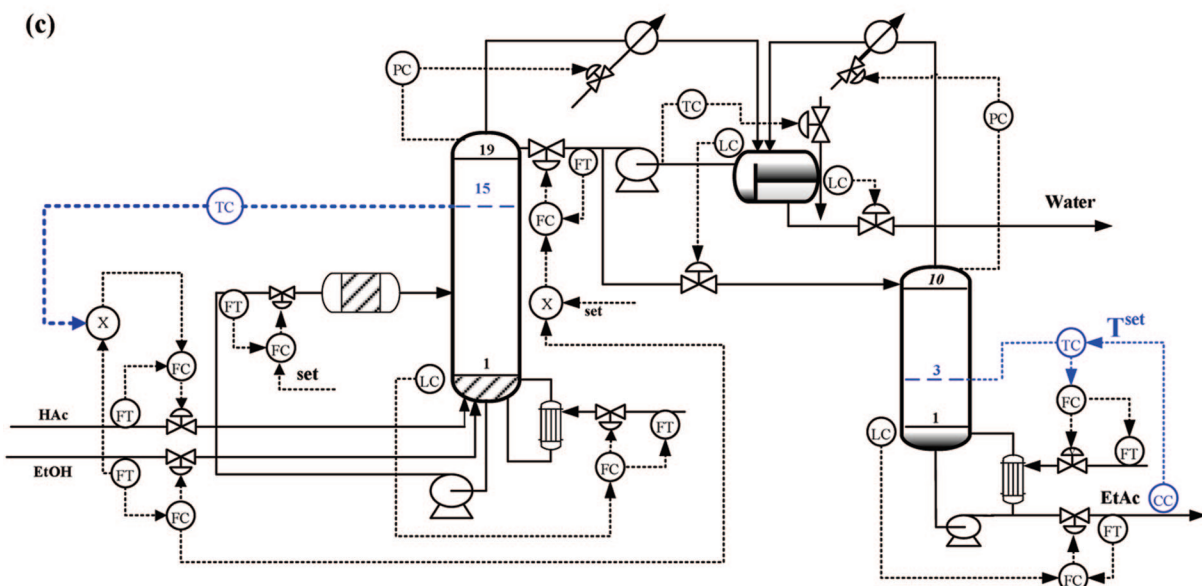


Figure 17. Control of the side reactor configuration (SRC) process: (a) CS1 (fixing RR), (b) CS2 (fixing R/F ratio), and (c) CS3 (CS2 with parallel cascade control on product purity).

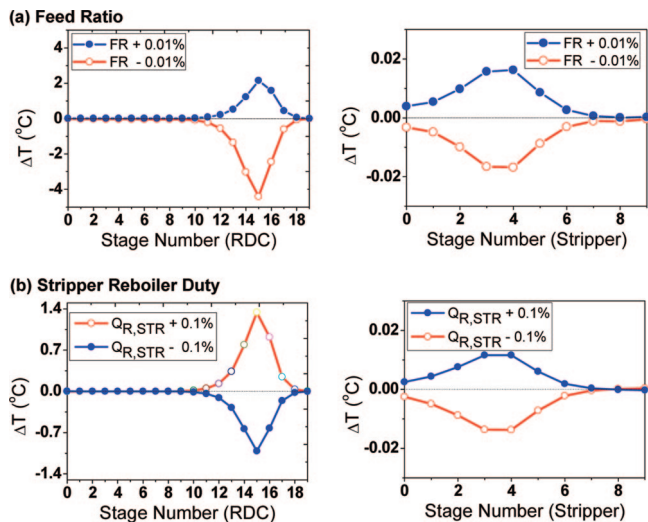


Figure 18. Sensitivities of tray temperatures for $\pm 0.1\%$ manipulated variables changes in CS1: (A) feed ratio changes and (B) stripper reboiler duty changes.

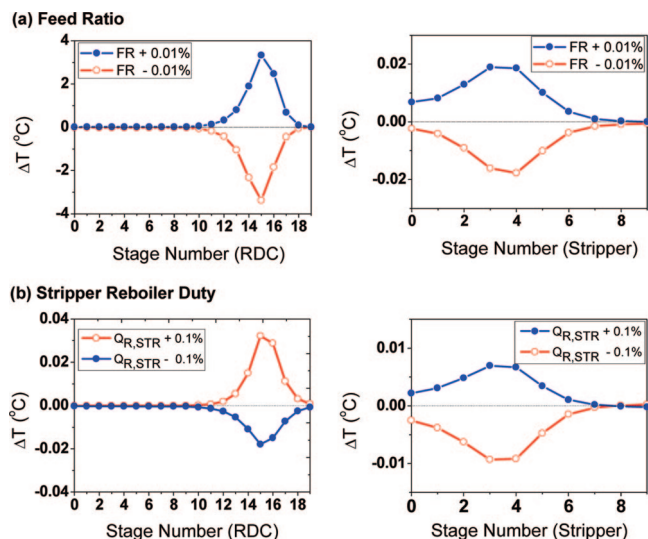


Figure 19. Sensitivities of tray temperatures for $\pm 0.1\%$ manipulated variables changes in CS2: (A) feed ratio changes and (B) stripper reboiler duty changes.

we use a temperature control to adjust the feed ratio ($F_{\text{HAc}}/F_{\text{EtOH}}$, FR). Thus, we have a 2×2 multivariable system and, from a unit-wise perspective, the pairing for the manipulated variables and the controlled variables are $FR-T_{\text{RD}}$ and $Q_{\text{R,STR}}-T_{\text{STR}}$. Before getting into controller design, we have one manipulated variable left, organic reflux flow rate (R). Two possible approaches can be taken: one is fixing the reflux ratio (RR), and the other is the ratio of the reflux to feed (R/F_{EtOH}). Therefore, we have two possible control structures: CS1 for keeping RR constant and CS2 for fixing reflux to feed ratio as shown in Figure 17.

4.2. Selection of Temperature Control Trays. Sensitivity analyses are performed for $\pm 0.01\%$ variations in the corresponding manipulated variables (FR and $Q_{\text{R,STR}}$), and the results are shown in Figure 18 for CS1 and Figure 19 for CS2. In both control structures an increase in $Q_{\text{R,STR}}$ leads to a decrease in the tray temperatures of the reactive distillation column due to a larger recycle flow rate for the reactive distillation column. As for the acid feed (FR) changes an increase in the heavy reactant results in the main column (RD column) tray temperature increase while the stripper temperatures show little

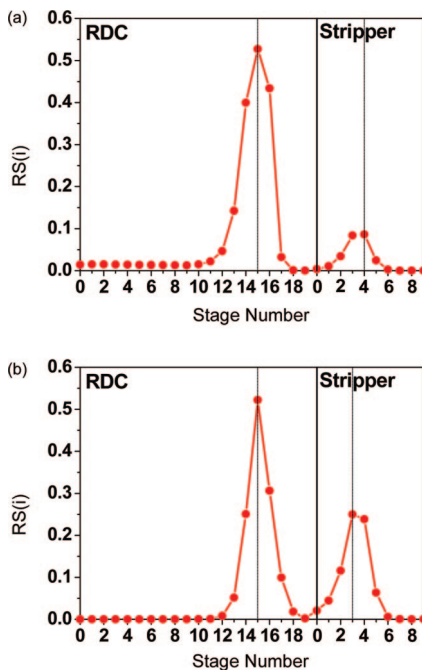


Figure 20. Row sums of NRG for RD column and the stripper for (a) CS1 and (b) CS2.

variation. At the completion of sensitivity analyses, the non-square relative gain (NRG²³) is used to find the temperature control trays in each column. The largest row sum of the NRG in each column is selected as the temperature control trays as shown in Figure 20. Note that the temperature control trays selected by the NRG are consistent with the most sensitive trays in Figures 18 and 19. The analyses select the temperature control trays: $T_{\text{RD},15}$ and $T_{\text{STR},4}$ for CS1 and $T_{\text{RD},15}$ and $T_{\text{STR},3}$ for CS2. Next, the relative gain arrays are computed for variable pairing (Table 3). They give the following controller pairing: CS1, $FR-T_{\text{RD},15}$, $Q_{\text{R,STR}}-T_{\text{STR},4}$; CS2, $FR-T_{\text{RD},15}$, $Q_{\text{R,STR}}-T_{\text{STR},3}$.

4.3. Controller Design. Once the decentralized control structure is in place, dynamic simulations are performed using Aspen Dynamics. A third-order 0.5 min time lag is assumed for temperature measurement,²⁴ and a dead time of 5 min is assumed for the composition analyzer. Liquid level is controlled using a proportional-only controller. Proportional-integral controllers are used for flow, pressure, composition, and temperature controls. Relay feedback tests²⁵ are performed on the temperature loops to find the ultimate gains (K_u) and ultimate period (P_u) of each temperature control loop, and initial controller parameters are calculated according to $K_c = K_u/3$ and $\tau_1 = 2P_u$. In order to obtain an acceptable damping, further detuning from the initial settings are required for some of the loops. Controller settings for all loops in CS1 and CS2 are summarized in Table 3.

4.4. Performance. The control performance is tested for feed flow and feed composition disturbances (ethanol and acetic acid). Figure 21 shows the dynamic responses of CS1 and CS2 for $\pm 20\%$ feed flow changes. The results show that the CS2 has fast (less than 5 h settling time) and symmetric responses, while the CS1 exhibits much slower (~ 10 h) and oscillatory responses. The reason for that is that we have severe interaction between the two process units (RD and stripper) for CS1 as compared to that of the CS2. This can be seen in Figures 18 and 19 when one compares the RD temperature sensitivity for the stripper reboiler duty changes or in the RGA values in Table 3. It can also be seen that with temperature control (CS1 and CS2) steady-state errors exist for both product compositions by 0.05%

Table 3. Variable Pairing, Results from Relay Feedback Tests, and Final Controller Settings

pairing	RGA	results of relay		control parameters	
		K_u	P_u (min)	K_c	τ_I (min)
CS1	$FR - T_{RD}$ $QR_{STR} - T_{STR}$	$T_{RD,15}$ $T_{STR,4}$	144.58 60.71	7.14 1.56	1.93 ^a 6.75 ^a 9.36 ^a
		$\Lambda = \begin{bmatrix} 0.67 & 0.33 \\ 0.33 & 0.67 \end{bmatrix}^{FR} Q_{R,STR}$			
CS2	$FR - T_{RD}$ $QR_{STR} - T_{STR}$	$T_{RD,15}$ $T_{STR,3}$	25.06 57.93	12.96 1.56	1.67 ^a 19.31 3.12
		$\Lambda = \begin{bmatrix} 0.98 & 0.02 \\ 0.02 & 0.98 \end{bmatrix}^{FR} Q_{R,STR}$			
CS3	$FR - T_{RD}$ $x_{B,EtAc} - T_{STR}^{SET}$ $QR_{STR} - T_{STR}$		27.22 16.92 57.93	12.24 19.32 1.56	0.91 ^a 5.64 9.65 ^a 244.8 ^a 38.64 6.24 ^a

^a Further detuning from the Tyreus–Luyben settings.

error for 20% production rate changes. For HAc feed composition disturbances (± 5 mol %) and EtOH feed composition disturbances (-5 and -10 mol %) the CS2 still works very

well with fast responses (Figure 22). The results clearly indicate that instead of fixing the reflux ratio it is preferable to fix the reflux to feed ratio, CS2, for this dual-temperature control for

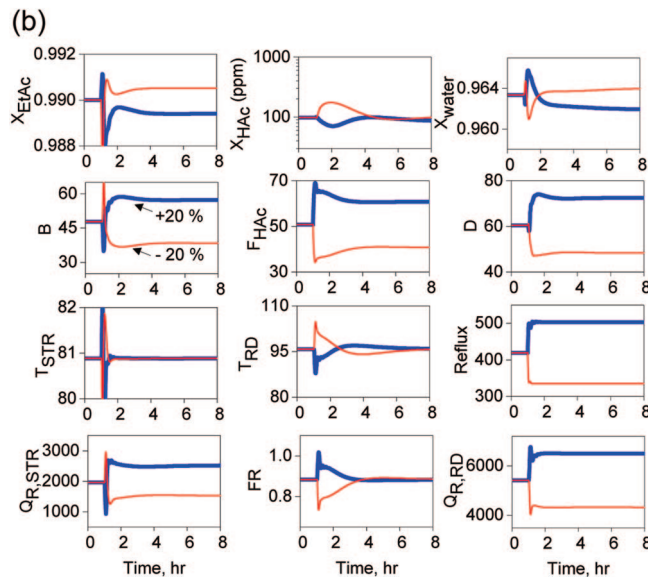
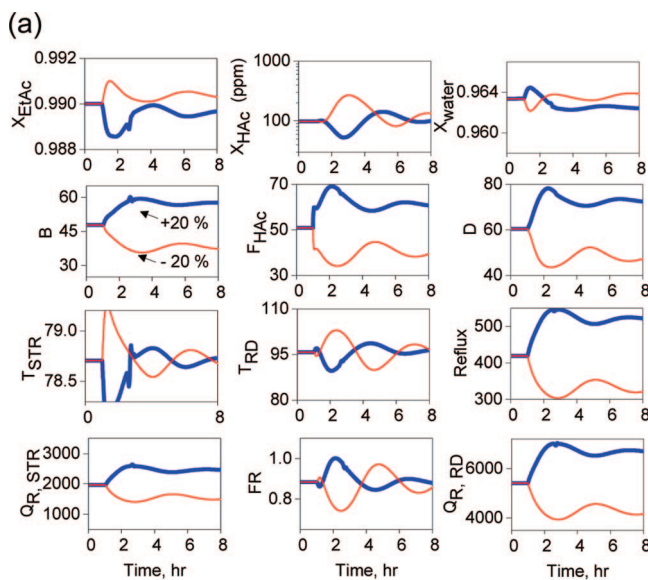


Figure 21. Load responses for $\pm 20\%$ production rate changes using (a) CS1 and (b) CS2.

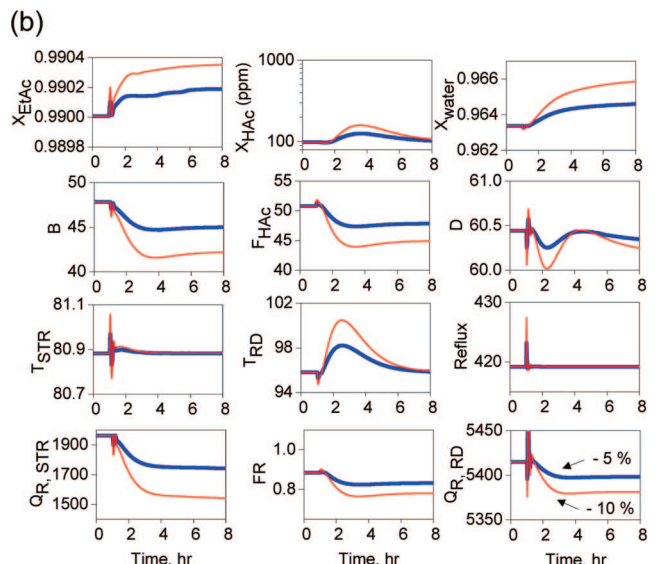
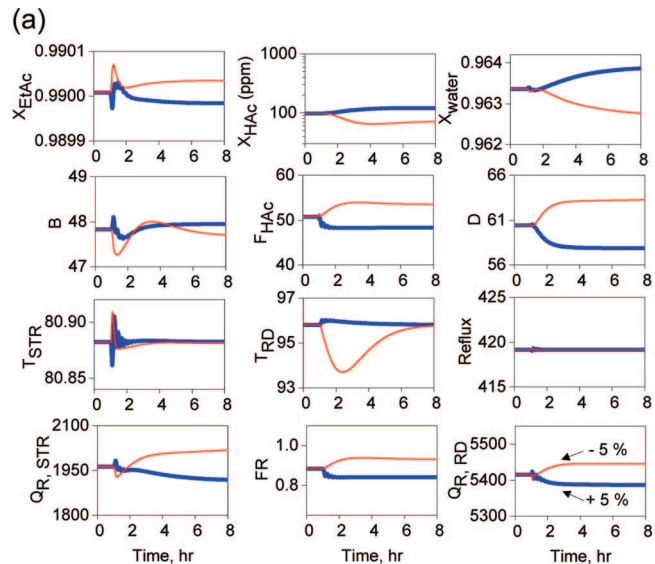


Figure 22. Load responses for feed composition disturbances using CS2: (a) ± 5 mol % HAc feed composition changes and (b) -5 and -10 mol % EtOH feed composition changes.

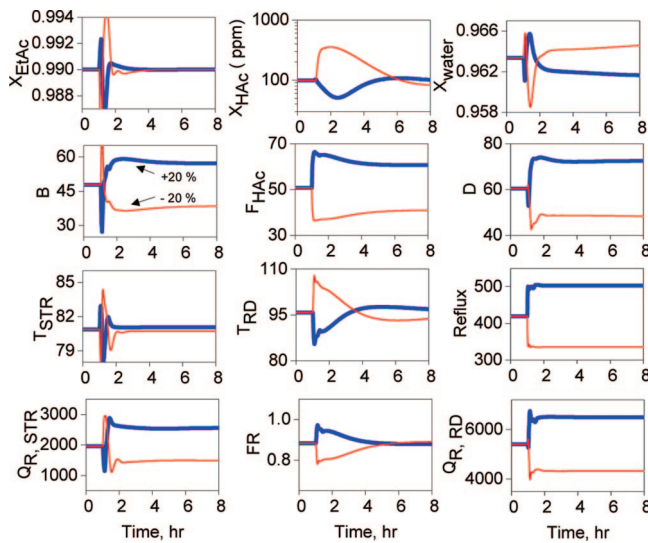


Figure 23. Load responses for $\pm 20\%$ production rate changes using temperature/composition cascade control (CS3) in the product purity loop.

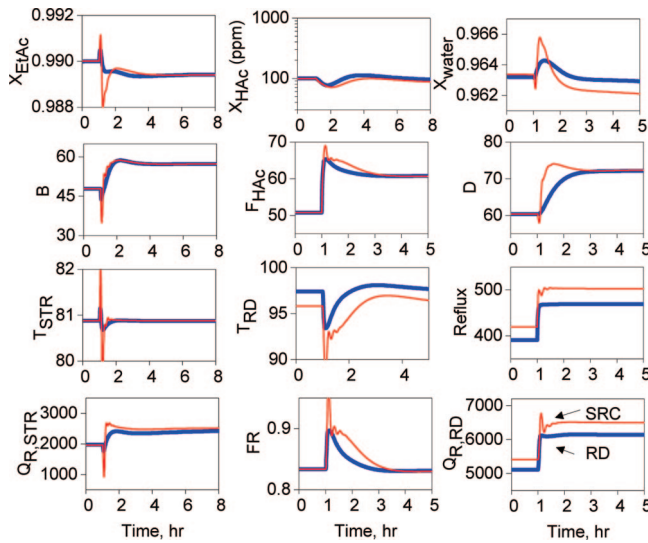


Figure 24. Load responses for 20% production rate increase using CS2 for (a) SRC and (b) RD.

the side reactor configuration. More importantly, reasonable control performance can be obtained using simple temperature control to handle production rate and composition variations.

4.5. Extension to Composition Control. To eliminate the steady-state offset in acetate purity, we also consider the composition control and use parallel cascade control; that is, the set point of the stripper temperature is reset by the output of the composition controller. Thus, we have one composition control, $x_{B,EtAc} - T_{STR}^{SET}$, and two temperature control, $Q_{R,STR} - T_{STR}$ and $Q_{R,RD} - T_{RD}$, at constant R/F_{EtOH} (named as CS3, as shown in Figure 17). Again, relay feed back tests are performed to find the ultimate gains (K_u) and ultimate period (P_u) of each control loop, and initial controller parameters are calculated according to $K_c = K_u/3$ and $\tau_1 = 2P_u$. Controller settings for all loops are summarized in Table 3. The control performance is tested for feed flow disturbance. Figure 23 shows the dynamic responses of 3 for $\pm 20\%$ feed flow changes. The control performance of CS3 is quite similar to that of the temperature control (CS2) except that steady-state error in product purity is eliminated.

4.6. Compared to RD Temperature Control. The steady-state economics of the side reactor configuration (SRC) is comparable to that of the reactive distillation (RD) while giving advantages in catalyst replacement and ease of maintenance. It will be interesting to see how the SRC dynamic behavior compared to that of the RD. Using the same control structure for both process configurations we compare the dynamic performance of SRC with that of RD. The CS2 have two temperature loops ($Q_{R,STR} - T_{STR}$ and $Q_{R,RD} - T_{RD}$) with a constant reflux to feed ratio (R/F_{EtOH}). The results, Figure 24, show that the speeds of responses for the compositions are about the same for both configurations. Unitwise, the RD shows a little smaller settling time in the main column, while the stripper exhibits a similar settling time.

5. Conclusion

In this work, acetic acid esterification using ethanol is used to illustrate design of the side reactor configuration (SRC). The SRC offers a maintenance advantage as compared to conventional reactive distillation. Instead of simultaneous design for the SRC, a gradual transition from the reactive distillation (RD) to a single reactive tray column (RD-SRT) and then to the side reactor configuration is demonstrated. The results show that the SRC is economically competitive with only a 5% increase in TAC and has a simple flow sheet structure with one external side reactor plus a reactive column base. Finally, the operability of the SRC process is tested for feed flow and feed composition disturbances. The results show that reasonable control performance can be obtained using simple temperature control schemes and the dynamic behavior is comparable to that of the RD.

6. Appendix A: TAC Calculation

Evaluation of equipment cost follows the procedure of Douglas²⁶ and the specific equations from earlier work.⁸ A payback period of 3 years is assumed and a M&S index of 1108.1 is applied in the calculation. Materials of construction are stainless steel. The equipment is sized as follows.

(1) Reboiler heat transfer area (A_R)

$$A_R[\text{ft}^2] = \frac{Q_R}{U_R \cdot \Delta T_R} \quad (\text{A1})$$

where Q_R [Btu/h] is the reboiler duty, the overall heat-transfer coefficient U_R is assumed to be 250 Btu/(h.ft²), and the temperature driving force ΔT_R [$^{\circ}\text{F}$] in the reboiler depends on the steam temperature.

(2) Condenser heat-transfer area (A_C)

$$A_C[\text{ft}^2] = \frac{Q_C}{U_C \cdot \Delta T_C} \quad (\text{A2})$$

where Q_C [Btu/h] is the condenser duty, the overall heat-transfer coefficient U_C is assumed to be 150 Btu/(h.ft²), and the log-mean temperature driving force ΔT_C [$^{\circ}\text{F}$] depends on the dew points and bubble points for a total condenser.

(3) Column length (L_C)

$$L_C[\text{ft}] = 2.4N_T \quad (\text{A3})$$

where N_T is the total number of trays. The capital and operating costs are calculated according to

(1) Column cost and reactor cost

$$\text{column cost}[\$] = \frac{\text{M \& S}}{280} (101.9D_C^{1.066} L_C^{0.802} (2.18 + F_C)) \quad (\text{A4})$$

where $F_C = F_m F_p = 3.67$.

(2) Tray cost

$$\text{tray cost}[\$] = \frac{\text{M \& S}}{280} (4.7 D_C^{1.55} L_C F_C) \quad (\text{A5})$$

where $F_C = F_s + F_t + F_m = 1 + 1.8 + 1.7$.

(3) Heat exchanger cost

$$\text{heat exchanger cost}[\$] = \frac{\text{M \& S}}{280} (A^{0.65} (2.29 + F_C)) \quad (\text{A6})$$

where $F_C = (F_d + F_p) F_m = (1.35 + 0) 3.75$ for the reboiler and $F_C = (F_d + F_p) F_m = (1 + 0) 3.75$ for the condenser.

(4) Steam cost

$$\begin{aligned} \text{steam cost}[\$/\text{year}] &= \frac{\$2.8}{1000 \text{ lb}} \times \left(\frac{Q_H}{924} \right) \\ &\quad \left(8150 \frac{\text{h}}{\text{year}} \right) \text{ for RD column} \end{aligned} \quad (\text{A7})$$

$$\begin{aligned} \text{steam cost}[\$/\text{year}] &= \frac{\$2.28}{1000 \text{ lb}} \times \left(\frac{Q_H}{969} \right) \\ &\quad \left(8150 \frac{\text{h}}{\text{year}} \right) \text{ for stripping column} \end{aligned} \quad (\text{A8})$$

(5) Cooling water cost

$$\text{cooling water cost}[\$] = \frac{\$0.03}{1000 \text{ gal}} \left(\frac{1 \text{ gal}}{8.34 \text{ lb}} \right) \left(\frac{Q_C}{30} \right) \left(8150 \frac{\text{h}}{\text{year}} \right) \quad (\text{A9})$$

(6) Catalyst cost

$$\text{catalyst cost}[\$] = \text{catalyst loading[lb]} \cdot 3.5 \frac{\$}{\text{lb}} \quad (\text{A10})$$

Acknowledgment

This work was supported by the China Petrochemical Development Corp., the Ministry of Economic Affairs, and National Taiwan University.

Abbreviations

EtOH = ethanol

EtAc = ethyl acetate

HAc = acetic acid

F_{HAc} = acid feed flow rate, kmol/h

F_{EtOH} = alcohol feed flow rate, kmol/h

F_d = factor for design type

F_m = factor for radiant tube material

F_p = factor for design pressure

FR = feed ratio ($F_{\text{HAc}}/F_{\text{EtOH}}$)

F_{ss} = flow rate of sidestream, kmol/h

K_{eq} = equilibrium constant for the hydrolysis reaction

K_u = ultimate gain

N_{RX} = number of trays in the reactive section

N_R = number of trays in the rectifying section

N_S = number of trays in the stripping section

N_{SR} = number of side reactors

$N_{ss,r}$ = location of sidestream return tray

N_{T3} = total number of trays in the third column

NRG = nonsquare relative gain array

P_u = ultimate period

Q_R = reboiler duty, kW

R = organic reflux flow rate, kmol/h

\mathcal{R} = reaction rate, kmol/s

T = reaction temperature, K

T_{RD} = selected temperature control tray in RD column

T_{STR} = selected temperature control tray in stripper

$T_{\text{STR}}^{\text{SET}}$ = set point of T_{STR}

TAC = total annual cost, \$1000/year

$W_{\text{cat},\text{bot}}$ = catalyst loading at column base

$W_{\text{cat},\text{RD}}$ = all catalyst loading for the original RD column design

$\%X_{\text{eq}}$ = achieving percentage of equilibrium conversion

k_F = forward rate constant, $\text{kmol}/(\text{s}^* \text{kg}_{\text{cat}})$

k_B = backward rate constant, $\text{kmol}/(\text{s}^* \text{kg}_{\text{cat}})$

m_{cat} = catalyst weight, kg

x_i = mole fraction for each component i

Greek Symbols

τ_I = integral time, min

Literature Cited

- Baur, R.; Krishna, R. "Distillation Column with Reactive Pump Arounds: An Alternative to Reactive Distillation". *Chem. Eng. Process.* **2004**, *43* (3), 435.
- Kaymak, D. B.; Luyben, W. L. Design of Distillation Columns with External Side Reactors. *Ind. Eng. Chem. Res.* **2004**, *43* (25), 8049.
- Kaymak, D. B.; Luyben, W. L. Optimum Design of A Column/Side Reactor Process. *Ind. Eng. Chem. Res.* **2007**, *46* (15), 5175.
- Jakobsson, K.; Pyhalohti, A.; Pakkanen, S.; Keskinen, K.; Aittamaa, J. Modelling of a Side Reactor Configuration Combining Reaction and Distillation. *Chem. Eng. Sci.* **2002**, *57* (9), 1521.
- Schoenmakers, H.; Buhler, W. Distillation Column with External Reactors - an Alternative to the Reaction Column. *Chem. Ing. Tech.* **1982**, *54* (2), 163.
- Gadewar, S. B.; Tao, L.; Malone, M. F.; Doherty, M. F. Process Alternatives for Coupling Reaction and Distillation. *Chem. Eng. Res. Des.* **2004**, *82* (A2), 140–147.
- Gangadwala, J.; Kienle, A. Minlp Optimization of Butyl Acetate Synthesis. *Chem. Eng. Process.* **2007**, *46* (2), 107.
- Tang, Y. T.; Chen, Y. W.; Huang, H. P.; Yu, C. C.; Hung, S. B.; Lee, M. J. Design of Reactive Distillations for Acetic Acid Esterification. *AIChE J.* **2005**, *51* (6), 1683.
- Lai, I. K.; Hung, S.-B.; Hung, W.-J.; Yu, C.-C.; Lee, M.-J.; Huang, H.-P. Design and Control of Reactive Distillation for Ethyl and Isopropyl Acetates Production with Azeotropic Feeds. *Chem. Eng. Sci.* **2007**, *62* (3), 878.
- Hangx, G.; Kwant, G.; Maessen, H.; Markusse, P.; Urseanu, I. Reaction Kinetics of the Esterification of Ethanol and Acetic Acid Towards Ethyl Acetate, Deliverable 22, Intelligent Column Internals for Reactive Separations (INTINT), Technical Report to the European Commission: 2001.
- Renon, H.; Prausnitz, J. M. Local Compositions in Thermodynamics Excess Functions for Liquid Mixtures. *AIChE J.* **1968**, *14*, 135.
- Hayden, J. G.; O'Connell, J. P. A Generalized Method for Predicting Second Virial Coefficients. *Ind. Eng. Chem. Process Des. Dev.* **1975**, *14* (3), 209.
- Yi, C. K.; Luyben, W. L. Design and Control of Coupled Reactor/Column Systems 0.1. A binary coupled reactor/rectifier. *Comput. Chem. Eng.* **1997**, *21* (1), 25.
- Yi, C. K.; Luyben, W. L. Design and Control of Coupled Reactor/Column Systems 0.2. More Complex Coupled Reactor/Column Systems. *Comput. Chem. Eng.* **1997**, *21* (1), 47.
- Yi, C. K.; Luyben, W. L. Design and Control of Coupled Reactor/Column Systems 0.3. A Reactor/Stripper with Two Columns and Recycle. *Comput. Chem. Eng.* **1997**, *21* (1), 69.
- Al-Arfaj, M. A.; Luyben, W. L. Comparison of alternative control structures for an ideal two-product reactive distillation column. *Ind. Eng. Chem. Res.* **2000**, *39* (9), 3928.
- Al-Arfaj, M. A.; Luyben, W. L. Comparative control study of ideal and methyl acetate reactive distillation. *Chem. Eng. Sci.* **2002**, *57* (24), 5039.
- Kaymak, D. B.; Luyben, W. L. Quantitative Comparison of Reactive Distillation with Conventional Multitunit Reactor/Column/Recycle Systems for Different Chemical Equilibrium Constants. *Ind. Eng. Chem. Res.* **2004**, *43* (10), 2493.
- Kaymak, D. B.; Luyben, W. L. Comparison of two types of two-temperature control structures for reactive distillation columns. *Ind. Eng. Chem. Res.* **2005**, *44* (13), 4625.
- Hung, S. B.; Lee, M. J.; Tang, Y. T.; Chen, Y. W.; Lai, I. K.; Hung, W. J.; Huang, H. P.; Yu, C. C. Control of different reactive distillation configurations. *AIChE J.* **2006**, *52* (46), 1423.

- (21) Chiang, S. F.; Kuo, C. L.; Yu, C. C.; Wong, D. S. H. Design Alternatives for the Amyl Acetate Process: Coupled Reactor/Column and Reactive Distillation. *Ind. Eng. Chem. Res.* **2002**, *41* (13), 3233.
- (22) Chien, I. L.; Teng, Y. P.; Huang, H. P.; Tang Yeong, T. Design and control of an ethyl acetate process: coupled reactor/column configuration. *J. Process Control* **2005**, *15* (4), 435.
- (23) Chang, J. W.; Yu, C. C. The relative gain for non-square multivariable system. *Chem. Eng. Sci.* **1990**, *45* (5), 1309.
- (24) Luyben, W. L.; Tyreus, B. D.; Luyben, M. L. *Plantwide Process Control*; McGraw-Hill, New York, 1998.
- (25) Shen, S. H.; Yu, C. C. Use of Relay-Feedback Test for Automatic Tuning of Multivariable Systems. *AICHE J.* **1994**, *40*, 627.
- (26) Douglas, J. M. *Conceptual Design of Chemical Process*; McGraw-Hill: New York, 1988.

Received for review December 03, 2007

Accepted September 19, 2008

IE071648O